Quota-Critical Witnesses

Experimental Signatures of the Action Limit

Part III of the Beyond the Ledger Series

Emiliano Shea

December 22, 2025

Abstract

We design three falsifiable experimental protocols to test Action Realism's central claim that physical reality is resource-bounded. We translate theoretical claims into falsifiable experimental protocols: (1) the *Simulation Complexity Witness*, which predicts increased compressibility and min-entropy degradation when a QRNG is driven beyond its action capacity; (2) *Ramsey Fisher Benchmarks*, which verify that Fisher information plateaus when the accumulated measurement record exceeds the apparatus ledger capacity N_{app}; and (3) *Ultra-Dense Fermi Gases*, which constrain the fundamental non-locality scale ℓ_0 via deviations in the equation of state. A positive result in any of these experiments would provide strong evidence consistent with Action Realism and motivate tighter bounds on the fundamental parameters of the unmeasurable substrate.

Contributions

- We design three falsifiable experimental protocols that test Action Realism's central claim that physical reality is resource-bounded.
- We operationalize "ledger capacity" N as a measurable hardware parameter (RAM+persistent storage), bridging theory and experiment.
- We provide quantitative falsification criteria and statistical methods for each witness, including explicit metrics (compression ratio, Fisher information plateau, EOS residuals).
- We propose a unified test protocol and experimental roadmap for cross-validating thermodynamic, metrological, and interaction limits.
- We synthesize evidence from generative AI, quantum metrology, and condensed matter physics into a unified Quota-Critical framework.

Contents

1 Introduction: The Paradigm of Quota-Criticality

The contemporary convergence of generative artificial intelligence, quantum information theory, and foundational physics provides a new operational lens and a family of metrics we can repurpose for physics experiments. This paradigm posits that the "realism" of an action—whether synthesized by a neural network or evolved by a Hamiltonian—is intrinsically defined by its adherence to finite resource quotas [3]. These quotas are not merely engineering constraints but are fundamental physical bounds: the thermodynamic cost of information erasure [5], the maximum rate of orthogonal state evolution [6], and the saturation of interaction strength in quantum fluids [4].

Action Realism refers to the hypothesis that physical processes are bounded by finite action budgets, with each distinct fact requiring minimum action $\hbar$.

1.1 Summary of Previous Results

In Paper I [9], we proved the Operational Bounded Diagonal Lemma and the Strict Resource Hierarchy, demonstrating that a finite physical system is operationally incomplete. In Paper II [8], we developed the mathematical architecture for the completion of this system: the Unmeasurable Sector $\mathcal{U} = \varprojlim \mathcal{S}_N$. We modeled $\mathcal{U}$ using Infinite Derivative Field Theory (IDFT) with a non-local kernel $e^{-\Box/M^2}$, showing that discrete bits (facts) emerge from this continuous substrate via the nucleation of topological defects called Folds. This paper translates those formalisms into experimental tests. Following Paper 2, we denote the unmeasurable sector as $\mathcal{U} = \varprojlim \mathcal{S}_N$.

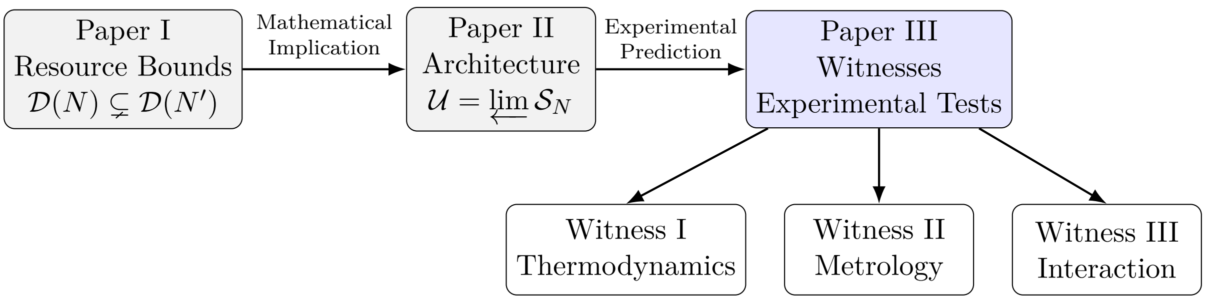

Figure 1: The three Quota-Critical Witnesses test complementary aspects of Action Realism: (1) **Thermodynamic limit**: maximum bit generation rate; (2) **Metrological limit**: maximum extractable information; (3) **Interaction limit**: fundamental non-locality scale. See Sections 3 to 5.

1.2 Why Three Witnesses?

A single experiment could always be explained away by domain-specific pathologies (e.g., thermal noise in thermodynamics or decoherence in metrology). By targeting three distinct regimes—thermodynamic bit generation, metrological information extraction, and many-body interactions—we construct a rigorous cross-check. A positive result in one domain might be an anomaly; consistent saturation across all three, tracking the same underlying action quota, would constitute robust evidence for Action Realism.

Notation Throughout this paper:

- $\hbar$ denotes Planck's constant (action quantum)
- N_{app} denotes apparatus ledger (controlled knob)
- N_{eff} denotes effective ledger (inferred)

- $N_{\max}$ denotes maximum configured bit capacity in a run (derived from FIFO depth $\times$ outcome-bitwidth)
- f_c denotes critical bit rate (Witness I threshold)
- ℓ_0 denotes fundamental non-locality scale (Witness III), where $\ell_0 = 1/M$ relative to Paper 2's mass scale.
- λ_F denotes the Fermi wavelength.

Key Experimental Signatures

- **Witness I (QRNG):** Compression ratio $\widehat{H}_{\mathrm{LZ}}$ exhibits change-point at $f = f_c$ tracking power budget P_{in}.
- **Witness II (Ramsey):** Fisher information $I_{\mathrm{FIFO}}(\phi)$ plateaus at $S_c \approx N_{\mathrm{app}} \cdot \hbar$, with linear shift vs. N_{app}.
- **Witness III (Fermi Gas):** EOS residuals with scaling $\Delta P \propto n^2 \epsilon_F$ yield a bound on ℓ_0 via Eq. (5.2).

2 Operational Definitions

We distinguish (i) *persistent* records, which remain available throughout the protocol without further stabilizing action, from (ii) ephemeral working memory.

Definition 2.1 (Ledger Capacity)**.** The ledger capacity N_{app} is operationally defined as the maximum number of persistent, recoverable classical bits that can be maintained within the experimental apparatus during the protocol's duration, given a fixed energy/action budget.

Definition 2.2 (Three Ledger Capacities)**.** We distinguish:

(i) **Apparatus ledger** N_{app}: persistent classical bits stored *within the device boundary* during acquisition (RAM + NVM with I/O sealed).

(ii) **Environment ledger** N_{env}: redundant classical copies deposited in uncontrolled degrees of freedom (e.g. stray photons, heat bath correlations).

(iii) **Effective ledger** N_{eff}: the maximum persistent record supported at fixed power, temperature, and isolation, estimated by calibration runs.

All witness thresholds are stated in terms of N_{eff} where applicable, with N_{app} as the controlled knob; in protocols where the apparatus memory is the dominant bottleneck we test the scaling directly in N_{app}.

Remark 2.3 (Calibration Protocol for N_{eff})*.* Operationally, N_{eff} is estimated by calibration runs in which known pseudo-random records are written and retained under identical power/temperature/isolation conditions. The maximum persistent record size is inferred from successful recovery probability over the protocol duration. By "I/O sealed" we mean the acquisition record is stored locally during the protocol and exported only after completion, with shielding/leakage tests bounding unintended external copies.

Detection Criterion A positive witness requires:

1. A pre-registered statistical test achieving $p < 10^{-3}$ and replicated change-point estimates across at least three independent devices/labs.
2. Within-lab repeatability across multiple days (fresh calibrations) with consistent breakpoint uncertainty.

Table 1: Comparison of Quota-Critical Witnesses. This table focuses on our three experimental protocols; see Table 2 for the broader cross-disciplinary context.

Witness	**Resource Tested**	**Key Metric**	**AR Prediction**
QRNG Complexity	Bit generation capacity	Compression ratio $\widehat{H}_{\mathrm{LZ}}$	Change-point at f_c
Ramsey Fisher	Information extraction	Fisher info $I_{\mathrm{FIFO}}(\phi)$	Plateau at $S_c \approx N_{\mathrm{app}}\hbar$
Fermi Gas EOS	Non-locality scale	Pressure residual ΔP	Bound via Eq. (5.2)

3. The regime boundary tracking a controlled ledger/resource parameter (e.g., N_{app}, P_{in}), not merely uncontrolled technical drift.

Table 1 summarizes the three witnesses and their predictions.

3 Witness I: Simulation Complexity Witness

This protocol tests the **Description–Action Link** (Paper I) in hardware. It frames the generation of quantum randomness not as a given, but as a process with a finite bit-production capacity governed by thermodynamic quotas [10].

3.1 Derivation

If each new stable classical bit requires a minimum action expenditure $\hbar$, then a physical random-bit source is not an oracle: it has a *bit-production capacity.* When driven beyond this capacity, the source must either (i) pay additional action (raising the ledger cost) or (ii) exhibit departures from ideal i.i.d. behavior.

3.2 The Protocol

We use a **Quantum Random Number Generator (QRNG)** based on photon arrival times (e.g., IDQ Quantis type).

1. **Fixed Power Budget.** Operate the QRNG with a fixed input power P_{in} (sweep range: 1 mW to 10 mW).

2. **Throughput Sweep.** Demand output bit rate f (range: 1 kHz to 100 MHz) while holding fixed all device resources.

3. **Operational Threshold.** Action Realism predicts a critical regime beyond f_c where measurable departures from ideal i.i.d. behavior emerge under predictor-limited tests.

4. **Analysis.** Analyze sample batches ($m = 10^6$ bits per rate) using online resource-bounded predictors P and Rényi min-entropy estimators.

5. **Artifact Audit.** Independently characterize detector dead-time, afterpulsing, and timing jitter versus f; exclude these as sources of apparent compressibility.

6. **Control Experiment.** Run a matched pseudorandom number generator (PRNG) through the same acquisition pipeline.

3.3 Predicted Signature

We monitor two scalar observables as a function of demanded throughput f: (i) a **predictor-based min-entropy estimate** $\widehat{H}_{\min}(f)$ (per-bit), and (ii) a **normalized code length** $\widehat{H}_{\mathrm{LZ}}(f)$ obtained from LZ77/LZMA-style compression on fixed-length blocks. We estimate $\widehat{H}_{\min}$ using an adversarial predictor class with bounded memory and compute per-bit min-entropy from empirical guessing probability (NIST-style predictor tests may be used as a secondary benchmark).

Compression Observable (implementation). We partition the bitstream into fixed blocks of length B (e.g. $B = 10^6$ bits) and compute

$$\widehat{H}_{\mathrm{LZ}} := \frac{|C(\mathrm{block})|}{B}, \tag{3.1}$$

where $|C(\mathrm{block})|$ is the compressed length in bits under a fixed compressor (e.g. LZMA at fixed settings). All runs use identical compressor version and settings; sensitivity is checked by repeating with a second compressor (e.g. zstd) as a robustness control.

Minimal scaling expectation. Under Action Realism we expect f_c to increase monotonically with input power, e.g. $f_c \propto P_{\mathrm{in}}$ up to device-specific efficiency factors.

Action Realism predicts a regime boundary near f_c where either $\widehat{H}_{\min}(f)$ drops or $\widehat{H}_{\mathrm{LZ}}(f)$ decreases (increased algorithmic compressibility and reduced predictor-limited min-entropy). We detect the boundary via change-point analysis (see Section 6.2 for statistical methods), and require that the inferred breakpoint tracks a controlled resource knob (e.g. input power P_{in} or enforced N_{app}) rather than temperature or detector dead-time.

Implementation Checklist: Witness I

- **Required Hardware**: Photon-arrival QRNG, tunable source/attenuator.
- **Controlled Knobs**: Throughput f, Power P_{in}.
- **Logged Variables**: Device temp, count rate, dead-time estimate.
- **Primary Statistic**: $\widehat{H}_{\mathrm{LZ}}(f)$ and $\widehat{H}_{\min}(f)$.
- **Primary Confounds**: Afterpulsing, dead-time, thermal drift.
- **Pass/Fail**: Change-point at f_c tracks P_{in} ($p < 10^{-3}$ or $P(\text{breakpoint in window}) > 0.99$).

4 Witness II: Ramsey Fisher Benchmarks

While Witness I tests bit generation, the Ramsey experiment tests **metrological limits**. It verifies that information extraction saturates when the ledger is full [7].

4.1 Derivation

We operationalize the accumulated action as

$$S_{\mathrm{total}} := \sum_{j=1}^{k} E_j \tau_j, \tag{4.1}$$

where (E_j, τ_j) are calibrated energy scales and interrogation times for each Ramsey segment. Here E_j may be taken as the calibrated energy scale of the active Hamiltonian during segment j (e.g. $\hbar\Omega_j/2$ for a driven qubit with Rabi rate Ω_j), or as the measured control-pulse energy delivered to the device; the analysis is repeated under both conventions as a robustness check. Recent work shows that Fisher Information (FI) does not grow indefinitely in sequential measurements but exhibits saturation linked to the finite memory of the probe. Action Realism predicts this saturation is fundamental to the ledger capacity.

4.2 The Protocol

1. **Prepare Probe.** Use a sequential non-adaptive Ramsey protocol on a spin ensemble.
2. **Variable Ledger.** Implement a FIFO buffer of k measurement outcomes using an FPGA with configurable depth $k = 2^8$ to 2^{16} (on-chip BRAM).
3. **Expend Action.** Vary the cumulative total action S_{total} expended.
4. **Measure.** Compute $I_{\text{FIFO}}(\phi)$ from the FIFO-limited record.
5. **Tracking.** Use Bayesian Hamiltonian Tracking [2] to attempt to optimize precision.
6. **Decoherence Control.** Independently measure T_2.

4.3 Predicted Signature

Action Realism. $I_{\text{FIFO}}(\phi)$ exhibits a plateau at action $S_c \approx N_{\text{app}} \cdot \hbar$. The smoking gun is a linear shift with N_{app}.

- We compare $I_{\text{FIFO}}(\phi)$ to an **online** estimator $I_{\text{online}}(\phi)$ that updates parameters without storing the full record; Action Realism predicts the plateau occurs in the FIFO-limited analysis at $S_c \sim N_{\text{app}}\hbar$ while the online estimator does not show the same N_{app}-locked breakpoint.

Falsification Criterion Action Realism is falsified for Witness II if the inferred plateau point $S_c/\hbar$ does not scale with N_{app} (regression slope consistent with 0 within error bars), or if the plateau is fully explained by decoherence (T_2) and technical-noise models across all values of N_{app}.

Implementation Checklist: Witness II

- **Required Hardware**: Trapped ion/spin ensemble, FPGA controller.
- **Controlled Knobs**: FIFO depth k (N_{app}), Action S_{total}.
- **Logged Variables**: T_2, clock stability, buffer usage.
- **Primary Statistic**: Fisher Information $I_{\text{FIFO}}(\phi)$.
- **Primary Confounds**: Decoherence, LO drift, estimator bias.
- **Pass/Fail**: Plateau S_c scales linearly with N_{app}.

5 Witness III: Ultra-Dense Fermi Gases

Finally, we look for a macroscopic signature in **condensed matter** using the Unitary Fermi Gas (UFG) [4].

5.1 Derivation

We parameterize the leading non-local correction phenomenologically as

$$\Delta P_{\text{nonlocal}}(n) = c_0\, \ell_0^3\, n^2\, \epsilon_F(n), \tag{5.1}$$

with c_0 an $\mathcal{O}(1)$ coefficient to be inferred or bounded. Here $\epsilon_F(n)$ denotes the local Fermi energy at density n.

5.2 The Protocol

1. **Platform.** Choose a fermionic system (^{6}Li) in an optical dipole trap ($T/T_F < 0.1$, density $n = 10^{13}$–10^{15} cm^{-3}).
2. **Sweep.** Measure the equation of state $P(n)$ via Bragg spectroscopy or in-situ density profiles.
3. **Analysis.** Perform a **Bayesian model comparison** (Bayes factor > 10) between standard local theory and the non-local model (see Section 6.2).

5.3 Predicted Signature

Action Realism. A non-local kernel induces systematic EOS residuals with density scaling $\Delta P \propto n^2 \epsilon_F$; a null result bounds ℓ_0 via Eq. (5.2).

$$\ell_0 \lesssim \left(\frac{\delta P}{|c_0|\, n^2 \epsilon_F} \right)^{1/3}, \tag{5.2}$$

where δP is the experimentally resolvable systematic residual after calibration to the best local EOS model.

Implementation Checklist: Witness III

- **Required Hardware**: Ultracold atom trap (^{6}Li or ^{40}K).
- **Controlled Knobs**: Interaction strength ($1/k_F a$), Density n.
- **Logged Variables**: Atom number, trap frequency, temperature.
- **Primary Statistic**: Pressure residual ΔP.
- **Primary Confounds**: Finite-T effects, trap anharmonicity.
- **Pass/Fail**: Bayes factor > 10 for non-local model.

6 Feasibility and Falsification

6.1 Timeline and Roadmap

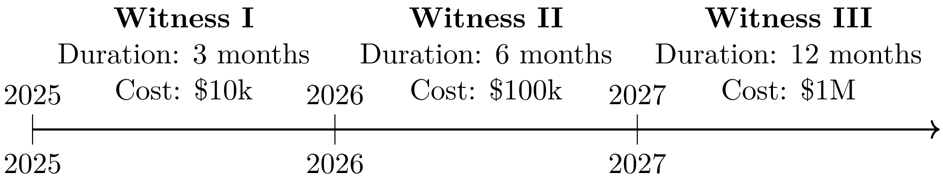

Figure 2: Experimental roadmap for the three Quota-Critical Witnesses. Witness I (QRNG complexity) requires modest resources and can be completed in months. Witness II (Ramsey Fisher) requires high-stability quantum systems. Witness III (Fermi gas EOS) demands precision many-body platforms. Progressive implementation allows early tests while building toward comprehensive validation.

As shown in Fig. 2, the experimental progression moves from desktop-scale tests to large-scale facility experiments.

6.2 Statistical Analysis

We use frequentist change-point significance for Witness I (time-series regime detection) and model-selection criteria (AIC/BIC or Bayes factors) for Witnesses II–III (competing parametric models); all analyses are pre-registered with fixed primary endpoints.

For each witness, we specify:

- **Witness I**: Segmented regression breakpoint significance via likelihood-ratio test with $p < 10^{-3}$, or a Bayesian change-point posterior with $P(\text{breakpoint in window}) > 0.99$.
- **Witness II**: AIC/BIC model comparison between linear-growth and saturating FI models.
- **Witness III**: Bayesian model comparison with Bayes factor > 10 (strong evidence).

6.3 Unified Test Proposal

A unified test would use a single quantum processor (e.g., trapped ions) to implement:

1. **QRNG mode**: Generate randomness via fluorescence detection (Witness I).
2. **Ramsey mode**: Perform sequential Ramsey interferometry (Witness II).
3. **Many-body mode**: Measure spin-spin correlations (Witness III).

This would test all three limits on identical hardware, controlling for system-specific effects.

7 Conclusion: The Final Compact

These three witnesses probe the Action Limit from three directions. Positive results would have profound implications:

- **Witness I Positive:** Quantum cryptography must account for bit generation limits.
- **Witness II Positive:** Quantum metrology standards need revision for memory bounds.
- **Witness III Positive:** High-density matter physics requires non-local corrections.

Null results also carry significant weight:

- **Null in I:** Establishes a lower bound on the sustainable bit-production capacity as a function of input power, constraining thermodynamic models of QRNG operation and motivating higher-precision entropy estimators.
- **Null in II:** Provides a constraint on any ledger-locked FI saturation, shifting the burden to decoherence-only explanations.
- **Null in III:** Yields a tight bound on ℓ_0 as a function of the EOS residual floor δP.

Beyond these specific implications, confirming Action Realism would require rethinking the foundations of quantum theory, moving from infinite Hilbert spaces to resource-bounded state spaces.

We invite experimental groups to implement these witnesses. Positive results in any would mark a paradigm shift; null results would place stringent bounds on resource-based interpretations.

Table 2: Taxonomy of Quota-Critical Witnesses across physics. Our three experimental witnesses (detailed in Table 1) target specific instances of these universal quota-critical phenomena.

Domain	**The Limit (Quota)**	**The Witness**
Generative AI	Kinematic Feasibility	Action Realism Metric [3]
Thermodynamics	Landauer Limit	Heat Dissipation [1]
Quantum Dynamics	Margolus-Levitin Speed	Orthogonal Evolution Time [6]
Condensed Matter	Unitarity ($\sigma_{\max}$)	Bertsch Parameter (ξ) [4]
Metrology	Finite Memory	Saturated Fisher Info [7]

A Resource Accounting for Witnesses

- **Witness I.** Persistent record: generated bitstream $R_{1:m}$ (~ 1 MB). Est. Cost: \$10k, 3 months.
- **Witness II.** Persistent record: FIFO buffer of k outcomes (~ 4 kB). Est. Cost: \$100k, 6 months.
- **Witness III.** Persistent record: set of calibrated (n, P) data points (~ 800 bytes). Est. Cost: \$1M, 12 months.

References

[1] Alexander B. Boyd et al. A metric for the entropic purpose of a system. *Physical Review Letters*, 132, 2024.

[2] Y. Ding et al. Efficient qubit calibration by binary-search hamiltonian tracking. *arXiv preprint arXiv:2501.05386*, 2025.

[3] S. Dwivedi et al. Generative action tell-tales: Assessing human motion in synthesized videos. *arXiv preprint arXiv:2512.01803*, 2025.

[4] Michael McNeil Forbes. The unitary fermi gas: An overview. *Proceedings of the INT Summer School*, 2012.

[5] Rolf Landauer. Irreversibility and heat generation in the computing process. *IBM Journal of Research and Development*, 5(3):183–191, 1961.

[6] Norman Margolus and Lev B Levitin. The maximum speed of dynamical evolution. *Physica D: Nonlinear Phenomena*, 120(1-2):188–195, 1998.

[7] Alireza Rezaakhani et al. Extractable information capacity in sequential measurements metrology. *Physical Review Research*, 5:043273, 2023.

[8] Emiliano Shea. The unmeasurable sector and the architecture of action. *Preprint*, 2025. Part II of the Beyond the Ledger Series.

[9] Emiliano Shea. Resource-bounded incompleteness: Operational limits in quota-bounded worlds. *Preprint*, 2025. Part I of the Beyond the Ledger Series.

[10] G. Toth et al. Dynamical landauer principle: Quantifying information transmission by thermodynamics. *Physical Review Letters*, 134:050404, 2025.